Visual Neuroscience (2006). **23**. 99–113. Printed in the USA.

DOI: 10.1017/S0952523806231092

Cloning and molecular characterization of cGMP-gated ion channels from rod and cone photoreceptors of striped bass (*M. saxatilis*) retina

CHRISTOPHE PAILLART,[1] KAI ZHANG,[2] TATIANA I. REBRIK,[1] WOLFGANG BAEHR,[2] AND JUAN I. KORENBROT[1]

[1]Department of Physiology, School of Medicine, University of California at San Francisco, San Francisco, California
[2]Department of Ophthalmology and Visual Sciences, Moran Eye Center, University of Utah Health Science Center, Salt Lake City, Utah

(RECEIVED August 19, 2005; ACCEPTED October 1, 2005)

Abstract

Vertebrate photoreceptors respond to light with changes in membrane conductance that reflect the activity of cyclic-nucleotide gated channels (CNG channels). The functional features of these channels differ in rods and cones; to understand the basis of these differences we cloned CNG channels from the retina of striped bass, a fish from which photoreceptors can be isolated and studied electrophysiologically. Through a combination of experimental approaches, we recovered and sequenced three full-length cDNA clones. We made unambiguous assignments of the cellular origin of the clones through single photoreceptor RT-PCR. Synthetic peptides derived from the sequence were used to generate monospecific antibodies which labeled intact, unfixed photoreceptors and confirmed the cellular assignment of the various clones. In rods, we identified the channel α subunit gene product as 2040 bp in length, transcribed into two mRNA 1.8 kb and 2.9 kb in length and translated into a single 96-kDa protein. In cones we identified both α (CNGA3) and β (CNGB3) channel subunits. For α, the gene product is 1956 bp long, the mRNA 3.4 kb, and the protein 74 kDa. For β, the gene product is 2265 bp long and the mRNA 3.3 kb. Based on deduced amino acid sequence, we developed a phylogenetic map of the evolution of vertebrate rod and cone CNG channels. Sequence comparison revealed channels in striped bass, unlike those in mammals, are likely not N-linked-glycosylated as they are transported within the photoreceptor. Also bass cone channels lack certain residues that, in mammals, can be phosphorylated and, thus, affect the cGMP sensitivity of gating. On the other hand, functionally critical residues, such as positively charged amino acids within the fourth transmembrane helix (S4) and the Ca^{2+}-binding glutamate in the pore loop are absolutely the same in mammalian and nonmammalian species.

Keywords: cGMP-gated ion channels, Retina, Photoreceptors, Rod, Cone

Introduction

The signal-transduction current in rod and cone receptors of the vertebrate retina arises from light-dependent changes in the activity of cyclic nucleotide-gated ion channels (CNG) located in the plasma membrane of the cell's outer segment (reviewed by Pugh & Lamb, 2000; Ebrey & Koutalos, 2001). The CNG channel protein from bovine rods was first purified by Cook et al. (1987) and its α subunit cDNA first cloned by Kaupp et al. (1989). Using this sequence as guide, CNG channels of rods and cones in several other species have now been cloned (reviewed by Kaupp & Seifert, 2002; Matulef & Zagotta, 2003). These proteins are members of a large gene family that also includes voltage-gated K^+ and HCN (Hyperpolarization-activated Cyclic Nucleotide-gated) ion channels (reviewed by Kaupp & Seifert, 2001; Hofmann et al., 2003). In addition to photoreceptors, changes in activity of CNG channels are part of the signal-transduction cascade in sensory neurons of the olfactory epithelium (reviewed by Zagotta & Siegelbaum, 1996; Zufall & Munger, 2001; Barry, 2003) and taste buds (Misaka et al., 1997; Lee et al., 2001; Sugita et al., 2004).

Rod and cone CNG channels are heteromeric complexes formed by an ensemble of α and β subunits. Each of these subunits can be broadly described to consist of six transmembrane helices, a pore loop and large cytoplasmic amino and carboxy terminal domains. The cyclic nucleotide-binding site in the carboxy terminus is connected to the last transmembrane segment of the channel by a characteristic linker peptide (C-linker) (reviewed by Kaupp & Seifert, 2002; Matulef & Zagotta, 2003). Heterologous expression of α subunits cloned from rods or cones yields functional channels

Address correspondence and reprint requests to: Juan I. Korenbrot, Department of Physiology, School of Medicine, Box 0444, University of California at San Francisco, San Francisco, CA 94143, USA. E-mail: juan.korenbrot@ucsf.edu

in various systems, but expression of β subunits alone does not yield active channels. The functional properties of heterologous α channels differ from those of native channels, for example, single-channel kinetics and L-cis-diltiazem sensitivity, yet coexpression of α and β restores native features to the heterologously expressed channels (rods: Chen et al., 1993; Korschen et al., 1995; cones: Gerstner et al., 2000).

Despite their broad structural similarities, CNG channels in rods and cones differ profoundly in several of their functional features. Photoreceptor CNG channels are permeable to both monovalent and divalent cations (rods: Colamartino et al., 1991; Zimmerman & Baylor, 1992; Tanaka & Furman, 1993; cones: Picones & Korenbrot, 1992; Haynes, 1995), but the Ca^{2+} to Na^{+} permeability ratio (PCa/PNa) is higher in cone than rod channels (Frings et al., 1995; Picones & Korenbrot, 1995*a*). Under normal physiological conditions, the fraction of the outer segment light-sensitive current carried by Ca^{2+} is about 35% in cones, but 20% in rods (Ohyama et al., 2000). The subunit stoichiometry of native channels in rods is 3α:1β (Zheng et al., 2002; Zhong et al., 2002; Weitz et al., 2002), but it is 2α:2β in cones (Peng et al., 2004). The cGMP dependence of channel activation in intact photoreceptors is modulated by Ca^{2+}, but in rods the modulation is small in extent and has a midpoint dependence on Ca^{2+} at about 20 nM (Sagoo & Lagnado, 1996; Nakatani et al., 1995), whereas in cones it is larger in extent and the midpoint on Ca^{2+} is at about 860 nM (Rebrik & Korenbrot, 1998; Rebrik et al., 2000). These functional differences are important in explaining, in part, the differences in the phototransduction signal between rods and cones in the same species (Korenbrot & Rebrik, 2002; Rebrik & Korenbrot, 2004).

To fully understand the structural basis of the functional differences between rod and cone CNG channels, it would be useful to compare the function of the channels in the native cells and in heterologous expression systems. This is not generally possible with available mammalian α and β subunits because in these species photoreceptor cells are small, and difficult to isolate and maintain in culture amenable to electrophysiological investigation. Furthermore, to understand the consequence of particular channel functional features to photoreceptor transduction, it would be useful to develop transgenic photoreceptors of altered channel function. Indeed, transgenic mouse rod and cone photoreceptors altered with respect to the expression of their α and β CNG subunits have been reported but, in both cell types, phototransduction is either absent or altered and photoreceptors eventually degenerate (Biel et al., 1999; Leconte & Barnstable, 2000; Huttl et al., 2005). Because of these reasons, we thought it valuable to clone and characterize the rod and cone CNG channels from striped bass retina.

In the retina of striped bass there is a rod-to-cone cell ratio of about 20:1 (Miller & Korenbrot, 1993). Functional rods and cones can be readily isolated from this retina, their electrical response to light has been characterized (Miller & Korenbrot, 1993), as well as a number of the biophysical features of their CNG ion channels (Picones & Korenbrot, 1995*a*; Hackos & Korenbrot, 1999; Ohyama et al., 2002). Bass cones can be single or twin pairs, each class distinguishable not only by their color sensitivity, but also by the kinetics and adaptation features of their photoresponse. Despite the differences in transduction features amongst cone subtypes, biophysical studies demonstrate that CNG ion channels are indistinguishable among the various cone types (Picones & Korenbrot, 1992; Picones & Korenbrot, 1995*b*). We report here the molecular structure of the bass rod, single and twin cone photoreceptor CNG channels. We analyze their nucleotide sequence and we report on the development of bio-tools for their biochemical and functional characterization. Knowing the structure of these channels will facilitate their cloning from other nonmammalian species, in particular zebrafish. Recent technical developments suggest it should be possible to generate altered CNG channels in transgenic zebrafish cone photoreceptors (Ivics et al., 2004).

Materials and methods

Animals, retinal cell dissociation, and collection of solitary cone photoreceptors

Striped bass (*Morone saxatilis*) were received from Professional Aquaculture Services (Chico, CA) and maintained in the laboratory in a small scale aquaculture facility under 14-h light/10-h dark light cycles. The UCSF Committee on Animal Research approved protocols for the upkeep and sacrifice of the animals. Under infrared illumination, solitary single and twin cone photoreceptors were obtained by gentle enzymatic proteolysis (collagenase and hyaluronidase, 0.5 mg/ml each) and mechanical shredding of a dark-adapted, isolated retina (Miller & Korenbrot, 1993). The resulting cell suspension was maintained in a Ringer's solution of the following composition (in mM); NaCl (143), KCl (2.5), $NaHCO_3$ (5), Na_2HPO_4 (1), $MgCl_2$ (1), $CaCl_2$ (1), HEPES (10), Minimum Essential Medium (MEM) amino acids and vitamins (Gibco-BRL, Rockville, MD), glucose (10). pH was 7.5 and osmotic pressure 310 mOsM.

In light, the cell suspension was deposited onto a glass coverslip that formed the bottom of a small tissue chamber (~200 μl volume) held on the stage of an upright microscope. The solution in the chamber was thoroughly perfused with Ringer's to remove cellular debris. Under microscopic observation, using DIC contrast enhancement and a TV camera and monitor, individual single and twin photoreceptor cells were collected using suction micropipettes maneuvered with a micromanipulator. The micropipettes used were fabricated from Corning 7740 glass capillary tubing (1.8/0.9 mm od/id) with a tip diameter only slightly larger than the width of solitary cells (8 μm for single and 14 μm for twin cones).

Individual cone photoreceptors were collected within the least possible volume (tens of picoliters) by gentle suction, the pipette withdrawn from the tissue chamber and its contents expelled under positive pressure into a 0.6-ml plastic tube containing 10 μl of a ice-cold hypotonic lysis buffer 10mM Tris-Cl, pH 8.0, 0.68 mM DTT with 0.5 U RNase inhibitor (Rnase Out, Invitrogen, Carlsbad, CA) in RNase-free water. After expulsion the pipette tip was broken in the same solution. Detergent was not used to prevent later inhibition of RT/PCR enzymes. The tube was immediately frozen on dry ice and stored at −76°C.

Retinal cDNA phagemid library

RNA was purified from retinas (with some attached pigment epithelium) isolated from light-adapted bass eyes. Freshly isolated tissue was immediately frozen under liquid nitrogen, pulverized and total RNA recovered using guanidium isothiocyanate (Chomczynski & Sacchi, 1987). mRNA was separated using oligo-dT cellulose chromatography and cDNA synthesized using reverse transcriptase with a mixture of oligo dT and random primers (Ausubel et al., 2005). A cDNA library was constructed in Lambda ZapII phagemid using standard protocols (Stratagene, La Jolla, CA). The library consisted of about $\sim 5 \times 10^7$ pfu.

Hybridization and PCR screening of phagemid library

The cDNA library was screened with two alternative methods: (1) low stringency plaque-hybridization to bovine rod α subunit (bCNGA1), a kind gift of Dr. U.B. Kaupp. (2) Recovery of PCR products synthesized using degenerate primers, GMP1 and GMP2, designed to hybridize to the conserved cyclic nucleotide binding domain GMP1(sense): 5′-CCIGGIGA(T/C)TA(T/C)AT(T/C/A)TG(T/C)(A/C)(A/G)IAA; GMP2(antisense): 5′-(A/G)CA(A/G)AAIA(A/G)(A/G)TCI(G/C)(A/T)(A/G)TAICC. The two methods yielded putative channel clones termed BassX and BassY.

BassX and BassY clones were originally incomplete and we used RACE amplification of retinal mRNA to synthesize the missing terminals. This was accomplished using the abridged universal amplification primer (AUAP) and nested gene specific primers. The N-terminus of BassX was amplified by two rounds of PCR using AUAP/bassX1 and AUAP/bassX2 (bassX1: 5′CTCTTCAAAACACGCCCTGGCA, bassX2: 5′-TGATCAGGGTCCAGTTGTA). The N-terminus of BassY was amplified by AUAP/bassY1 (bassY1: 5′-ATGGTCCAGTTGTACATTACTG). Full-length BassX and BassY cDNAs were subcloned into pCR2.1-TOPO vector (Invitrogen) and sequenced from both ends.

BassZ was cloned from bass retina cDNA library through two rounds of PCR amplification using primers designed based on the sequence of the mouse cone β subunit (Gerstner et al., 2000). First round PCR was performed with primers bassZ1 (5′ (A/G)AT(T/C/A)(T/C)T(A/G)GTNCA(T/C)TA(T/C)CC) and M13 (reverse). The PCR product was used as template for a second PCR round with primers bassZ2 (5′-T(T/C)CCNCCNAA(A/G)GA(A/G)GA(A/G)ACNCC) and T3 (reverse). To obtain the full ORF, the incomplete clone was amplified using both 5′ and 3′RACE. It was then subcloned into pCR2.1-TOPO vector and completely sequenced in both directions.

In-situ hybridization

In-situ hybridization was used to identify retinal cells expressing candidate CNG ion channels cDNA clones. Hybridization was carried with small modifications of the procedures originally described by Raymond et al. (1993). Dark-adapted striped bass eyes were hemissected, eyecups incubated 10 min in Ringer's solution containing 3 mg/ml each hyaluronidase and collagenase and then fixed by immersion in 4% paraformaldehyde in Ringer's. After fixation, the eyecup was infiltrated with OCT through slow successive exchanges with sucrose:OCT mixtures. The infiltrated eyecup was frozen and 10 μm naso-temporal sections cut parallel to the equator using a freezing microtome. Sections were attached to Superfrost/Plus glass slides (Fisher, Pittsburg, PA) and successively reacted with 0.1 M triethanolamine (pH: 8.0) and 0.1 M triethanolamine/0.25% acetic anhydride, dehydrated, and incubated overnight in a humid chamber at 56°C with hybridization medium consisting of 50% formamide, 10% dextran sulfate, 1× Denhardt's solution, 1% w/v blocking reagent (Roche, Indianapolis, IN), 300 mM NaCl, 1 mM EDTA, 10 mM Tris-HCl pH 7.5 containing 5 μg/ml of denatured RNA probes.

To produce BassX and BassY probes, 300 bp long stretches from the respective cDNA clones were first PCR amplified and then subcloned into the SrfI site of pCR-ScriptTM SK (+) vector (Stratagene). The primer pairs used in these amplifications were (1) bassX3 (5′-AACACCTACTACTACTGGC-3′) and bassX4 (5′-GTGATGCCGAATACGAGGT-3′). (2) bassY2 (5′-ATTTGTATTACAACTGGCTGTTC-3′) and bassY3 (5′-GTCAAAGCCATAGTAGAAA-3′). Proper vector structure was confirmed by sequencing from both ends. RNA probes were labeled with digoxigenin (DIG RNA Labeling kit, Boehringer Mannheim/Roche, Germany) using either T3 or T7 RNA polymerase for sense and antisense probes, respectively.

Following overnight incubation with RNA probes, slides were rinsed several times with 2 × SCC at room temperature, 2 × SCC + 50% formamide at 60°C, 2 × SCC at 37°C, and incubated with 20 μg/ml of RNase A for 30 min. Sections were then incubated for 2 h in 100 mM Tris-HCl pH 7.5, 150 mM NaCl, 0.2% Tween-20, and 1% blocking reagent (Roche). cRNA hybrids were identified following overnight incubation at 4°C with anti-digoxigenin antibody conjugated to alkaline phosphatase (1:100, Roche). The presence of alkaline phosphatase was revealed after overnight incubation at room temperature with NBT/BCIP (Vector Labs, Burlingame, CA).

Single-cell RT-PCR

Cells were lysed by twice thawing and freezing the 0.6-ml plastic tube holding contents of the suction micropipette. Cellular debris was pelleted by centrifugation and first-strand cDNA synthesized in the supernatant with Sensiscript Reverse Transcriptase (Qiagen, Valencia, CA) using Oligo (dT)12–18 as primer (Invitrogen). We added to each reaction tube 10 μl of a master mix consisting of 2 μl 10× buffer RT, 2 μl dNTP mix (5 mM each dNTP), 1 μl Oligo (dT) 12–18 (0.5 μg/μl), 0.25 μl Rnase Out (40 Units/μl), 1 μl Sensiscript Reverse Transcriptase, and 3.75 μl Rnase-free water. After 1 h synthesis at 37°C, the mixture was heated to 93°C for 5min (to inactivate the RT enzyme) and then stored at 4°C.

We performed two rounds of PCR amplification using HotStar Taq DNA polymerase (Qiagen) in a final 50 μl PCR buffer and reactants. 5 μl of reverse transcribed cDNA was used as DNA template in the first round PCR and 1 μl of the PCR product was used in the second round PCR. The HotStar Taq DNA polymerase was activated at 95°C for 15 min. Typically, we used 30 PCR cycles each consisting of 30 s periods at 94°C, 30 s at the appropriate annealing temperatures (Ta) and 1 min at 72°C. In the final cycle, the 72°C step was sustained for 11 min.

For DNA amplification of BassX, we used a nested PCR. For the first round PCR, the forward primer was bassX5 (5′-GGAGAAAAAGGAGAGGAAGG-3′), the reverse primer was bassX6 (5′-GAGGTTGGAGATACGGAGAG-3′). The computed value of the midpoint of the annealing curve (Ta) was 51°C for both primers. For the second round PCR, the forward primer was bassX7 (5′-ACTGGCTGGCTATCATCAC-3′), the reverse primer was bassX8 (5′-GTGATGCCGAATACGAGGT-3′). The computed Ta for both primers was 54°C. The expected size of the amplicon was 299 bp. For DNA amplification of BassY, we used the same pair of primers for both rounds of PCR. The forward primer was bassY4 (5′-TGTATTACAACTGGCTGTTC-3′) and the reverse primer was bassY5 (5′-GTCAAAGCCATAGTAGAAA-3′); the Ta was 51°C for the first round and 54°C for the second round. The expected amplicon size was 308 bp. For DNA amplification of BassZ, we used the same pair of primers in both PCR rounds. The forward primer was bassZ3 (5′-CTGCTGCTCCTGAAAATCC-3′) and the reverse primer was bassZ4 (5′-ACCCTGTCCATCTTGCTCTC-3′). The Ta was 60°C and the expected size of the amplicon was 457bp. PCR products were size separated by electrophoresis on horizontal 2% agarose gels. Discrete bands were excised, DNA recovered (QIAquick kit, Qiagen) and sequenced.

As positive control for the efficiency of the RT-PCR process, we used authentic channel cRNA as starting material and processed it in parallel with single cell samples. cRNA was produced from the BassX cDNA cloned into pcDNA3.1. Capped cRNA was produced using AmpliCap T7 kit (Epicentre, Madison, WI) and plasmid DNA was hydrolyzed with DNase 1. Through calibration of the yield of RT-PCR products, we determined that 30 fg of channel cRNA yield approximately the same amount of amplified DNA as a single photoreceptor.

Single-cell immunocytochemistry

Freshly isolated, intact, and unfixed photoreceptors were labeled with polyclonal antibodies generated in rabbits against peptides specific to the rod or cone CNG α subunits. Polyclonal antibody anti-rod α CNG (named bassRod), was generated with the KLH-conjugated peptide: CPALDDPDEPAFGEP (amino acids P282–P295). Polyclonal anti-cone α CNG antibody (named bassCone), was generated with the KLH-conjugated peptide: CRFVYPDPAD-PEFGR (amino acids R303–R316). Antibodies were purified by affinity chromatography using the same BSA-conjugated peptides. Cells were dissociated from a dark-adapted retina as described above. The cell suspension in Ringer's solution was delivered onto a ConcanavalinA-coated glass coverslip held on a tissue culture well. After 10 min at room temperature, the glass coverslip was submersed in 2 ml of Ringer's solution containing BSA (5 mg/ml) and the primary antiCNG antibody (~1 mg/ml stock) (antiRod 1:100, or antiCone 1:40). 30 min later the incubating solution was gently exchanged several times with BSA-Ringer and the coverslip then immersed in 2 ml of BSA-Ringer now containing a fluorescent labeled, anti-rabbit antibody (1:50, Cy3 labeled, Jackson Immuno Research Labs, West Grove, PA or Texas-Red labeled, Molecular Probes, Eugene, OR). After 30-min incubation, the coverslip was gently washed several times with BSA-Ringer and observed under an epifluorescent microscope with a 40×, 0.75 NA water immersion objective.

RNA blots

Total bass retinal RNA was isolated using guanidium isothiocyanate (Chomczynski & Sacchi, 1987) and was then denatured and size separated by electrophoresis on a 2.2 M formaldehyde/1% agarose gel (20 μg RNA/lane). The RNA size was estimated through the use of RNA ladder (0.24–9.5 kb, BRL). RNA fragments were blotted onto charged nylon membranes by capillary transfer and cross-linked by UV light irradiation. Specific mRNAs for each of the genes of interest were identified in the blots by high stringency hybridization to RNA probes.

To identify BassX and BassY RNA messages, ^{32}P-labeled RNA probes were synthesized from the same pCR-ScriptTM SK (+) vector (Stratagene) detailed above under *in-situ* hybridization. Hybridization was carried out at 42°C for 12 h in 5× SSPE, 5X Denhardt's, 0.5% sarcosyl, 50% formamide and 200 μg/ml salmon sperm DNA. The blot was washed at progressively higher stringencies up to 0.1× SSC/0.1% SDS at 60°C.

To identify BassZ RNA message, digoxigenin-labeled DNA probes were synthesized from the channel cDNA clone. 457-bp long probes were synthesized by PCR using the same primers used in the single cell RT-PCR experiments (bassZ3 and bassZ4, see above). Hybridization was carried out at 45°C for 24 h in 5X SSC, 5X Denhardt's, 0.5% sarcosyl, 50% formamide and 100 μg/ml each sheared salmon sperm DNA and tRNA. The blot was washed at progressively higher stringencies up to 0.5X SSC/0.1% SDS at 60°C. The location of the dig-labeled probe was identified with anti-dig antibody conjugated to alkaline phosphatase, and a phosphatase chemiluminescent substrate (CDP-*Star*, Roche)

Protein blots

Dark-adapted retinas were isolated under infrared illumination, and immediately frozen in liquid N_2. The frozen tissue was pulverized under liquid N_2, immediately homogenized in loading buffer: 50 mM Tris-HCl, pH 6.8, 10% glycerol, 0.5% SDS, and then heated to 90°C for 5 min. The homogenate was centrifuged at 25,000*g* for 5 min at 4°C and the supernatant collected and stored. Proteins in the supernatant were separated in 7.5% polyacrylamide SDS-PAGE and then electro-transferred to PVDF membranes. The protein blot was incubated overnight at 4°C in blocking solution consisting of PBS with 0.1% Tween20, 3% dry milk, 2.5% goat serum, and 50% sea-block (Pierce, Rockford, IL), followed by 4 h incubation at room temperature with primary antibody diluted in blocking solution (1:4,000) (~ 1 mg/ml stock). After repeated washing in blocking solution, the blot was incubated in secondary antibody for 3–4 h at room temperature. The secondary antibody was anti-rabbit/goat IgG conjugated to horseradish peroxidase (Jackson ImmunoResearch Labs, West Grove, PA) diluted 1:10,000 in blocking solution, now containing 2.5% fish serum (East Coast Biologics, North Berwick, ME) instead of sea-block. The secondary antibody was detected using a chemiluminescent HRP substrate (ECLplus, Amersham, Piscataway, NJ).

BioInformatics

To analyze the structure of bass CNG channels we used a Web-based analytical tool [http://workbench.sdsc.edu, Subramanian (1998)] and compared it to the following available sequences (UniProt, http://www.pir.uniprot.org accession number in parenthesis). Rod α subunit (CNGA1): human (P29973), bovine (Q00194), canine (Q28279), mouse (P29974), rat (Q62927), and chicken (Q90980). Cone α subunit (CNGA3): human (Q16281), bovine (Q29441), mouse (Q9JJZ8), rat (Q9ER33), chicken (Q90805), and goldfish (Q80416). Rod β subunit (CNGB1): human (Q14028), bovine (Q28181). Cone β subunit (CNGB3): human (Q9NQW8), canine (Q8MJD7), mouse (Q9JJZ9). Drosophila eye CNG channel (Q24278). Multisequence alignment was executed using ClustalW3.2. Phylogenetic inferences were made using PHYLIP v 3.6 (http://evolution.genetics.washington.edu/phylip.html). This is a comprehensive collection of algorithms to implement various probabilistic models of molecular evolution discussed in detail by Felsenstein (2004), the program developer.

Results

Through a combination of techniques, we identified in striped bass retina three cDNA clones (BassX, BassY and BassZ) recognized as putative CNG ion channels by sequence homology to cloned mammalian channels. Briefly, BassX was recovered by low stringency screening of a cDNA library with bovine rod CNG α subunit probe (Kaupp et al., 1989). BassY was identified through PCR screening of retinal mRNA using degenerate primers designed to complement sections of the consensus cyclic nucleotide binding domain. BassZ was recovered through PCR screening of a cDNA retinal library using degenerate primers designed to complement specific sections of the mouse cone CNG β subunit (Gerstner

et al., 2000). In every instance, incomplete clones were RACE extended at their 3′ and/or 5′ ends using retinal mRNA as substrate. Finally, complete coding sequences were verified to be contiguous using N-terminal and C-terminal primers.

Cellular assignment of cloned sequences

In the retina, CNG ion channels are expressed in photoreceptors and also in ganglion (Ahmad et al., 1994) and bipolar cells (Henry et al., 2003). Sequence homology and the cloning protocol suggested BassX and BassY are α subunits, and BassZ is a β subunit. To determine the cell of origin of the cloned channels we first carried out *in-situ* hybridization of RNA probes to frozen, fixed striped bass retinal sections.

In-situ hybridization

Putative α subunits BassX and BassY sequences are particularly distinct in their N-terminal region. Therefore, we synthesized two cRNA probes, designed to distinguish the subunits from each other. The probes include regions encoding amino acids Y137-G246 in BassX (330 bp) and Y112 to G212 in BassY (303 bp). In both clones the probes encompass approximately from the start of transmembrane helix 1 to the end of helix 3. RNA probes were labeled with digoxigenin and their localization revealed through immunohistochemistry using anti-digoxigenin antibody conjugated to alkaline phosphatase. Typical results are illustrated in Fig. 1. As a positive control, we also tested hybridization of a bass rhodopsin (a gift of Dr. B. Burnside, UC Berkeley). As expected, rhodopsin mRNA is expressed in the outer nuclear layer of the bass retina (data not shown), where rod nuclei are aligned in 3 to 4 rows (Fig. 1). Antisense CNG RNA probesX and Y heavily labeled the outer nuclear layer, while sense probes did not (Fig. 1 BassX and BassY). However, hybridization failed to distinguish rod from cone nuclei; cone nuclei are preferentially located in the most distal row, immediately next to the inner segment (Fig. 1). The same probes, nonetheless, hybridize to distinct mRNA molecules when tested in RNA blots at high stringency (see below). Failure to recognize rods from cones is almost certainly due to the inability to reach sufficient stringency in the tissue when compared with the stringency that can be achieved in RNA blots.

The antisense BassX channel probe, while unable to distinguish rod from cone nuclei, did label some cells in the inner nuclear layer (INL) (Fig. 1). The label, however, was faint and not homogeneous. Since bipolar cells in goldfish retina express a cone-specific CNG ion channel (Henry et al., 2003), the irregular inner nuclear layer (INL) label may identify these neurons. Antisense BassY probe, on the other hand, did not label the INL or ganglion cell (GC) layers significantly different than sense probes. Thus, while results of *in-situ* hybridization did not allow us to specifically assign clones BassX or BassY to either rods or cones, they indicate the expression level of CNG channels in non-photoreceptor retinal cells is much, much less than in the photoreceptor cells.

Single-cell RT-PCR

We made unambiguous assignments of cDNA clones as rod or cone in origin through single-cell RT-PCR. Mechanically shredding the bass retina yields isolated single and twin cones. These cells, however, are not complete: they lack nuclei and synaptic pedicles. Nonetheless they are viable and continue to respond to light for several hours in short term culture (Miller & Korenbrot, 1993). Rods, on the other hand, are almost exclusively present as outer segment with a small remnant of the mitochondrial-rich ellipsoid bag. The absence of nuclei in isolated cones is advantageous because we did not have to contend with genomic DNA contamination within the collected cells. A challenge in our experimental design, however, is that the medium in which photoreceptors are initially isolated can be rich in genomic DNA from injured cells. Carelessly collecting suspension medium can cause false-positive results. To minimize this possibility, isolated photoreceptors were held in a small volume tissue chamber on a microscope stage and the bathing medium in the chamber exchanged extensively before individual cells were collected with suction micropipettes. This washout both removed cellular debris and potential contaminating genomic DNA. We produced cDNA from individual single or twin cones using oligo dT primers and reverse transcriptase (RT) and then amplified this material using Taq polymerase (PCR). Also, we processed side-by-side samples collected from the tissue chamber but which did not contain individual photoreceptors (we call them "sham" samples). We only analyzed samples collected under conditions where the "sham" did not yield any PCR product.

Shown in Fig. 2 are typical images of ethidium-bromide-stained agarose gels run at the end of the single-cell RT-PCR. In each gel lane are products of reactions run side-by-side in individual single (S) or twin (T) cones, as well as negative and positive controls. In Panels A and B are typical results of reactions carried out with probes specific to the BassX. Positive control was an RT-PCR reaction carried out with RNA synthesized with DNA-dependent RNA polymerase from BassX cDNA (lane X). As expected a single amplicon of about 300 bp is observed (anticipated size 299 bp). Negative controls were the RT-PCR reactions carried out on a "sham" sample (lane M), distilled water (lane W) or Ringer's (lane R). As expected, there was no reaction product in the negative controls. Both single and twin cones, but not every cell sample, yielded a single reaction product of the expected 300 bp size. Individual failures are almost certainly technical in nature reflecting mRNA degradation. The reaction product was sequenced and it was, in every instance, the sequence anticipated from the BassX clone. The results indicate that both single and twin cones express the BassX clone. That is, BassX is the cone CNG α subunit (sbCNGA3).

In Fig. 2, Panel C is shown the image of a gel with the reaction products obtained from single-cell RT-PCR carried out with probes specific to the BassY clone. There was a reaction product in the positive control (lane X), RNA from BassX clone, about 300 bp in size, as anticipated from the sequence (299 bp). There were no reaction products in any of the negative controls: "sham" (lane M), distilled water (lane W) or Ringer's (lane R). Every one of the individual cones tested, single (S) or twin (T), failed to yield a PCR reaction product. These results allow us to conclude that neither single nor twin cones express the BassY clone.

The logic of the results in Fig. 2 indicates that clone BassY is the rod CNG α subunit (sbCNGA1). This is because *in-situ* hybridization data show that BassY is photoreceptor specific, and single-cell RT-PCR results indicates it is not expressed in cones. This logical conclusion was confirmed through studies with specific antibodies detailed below.

BassZ was recognized as a putative CNG β subunit by homology to known mammalian channel sequences. We identified BassZ to be cone specific through single-cell RT-PCR. In Fig. 3, panels A and B are shown results of a typical experiment in which expression of BassZ was assessed in single and twin cones. Illustrated is

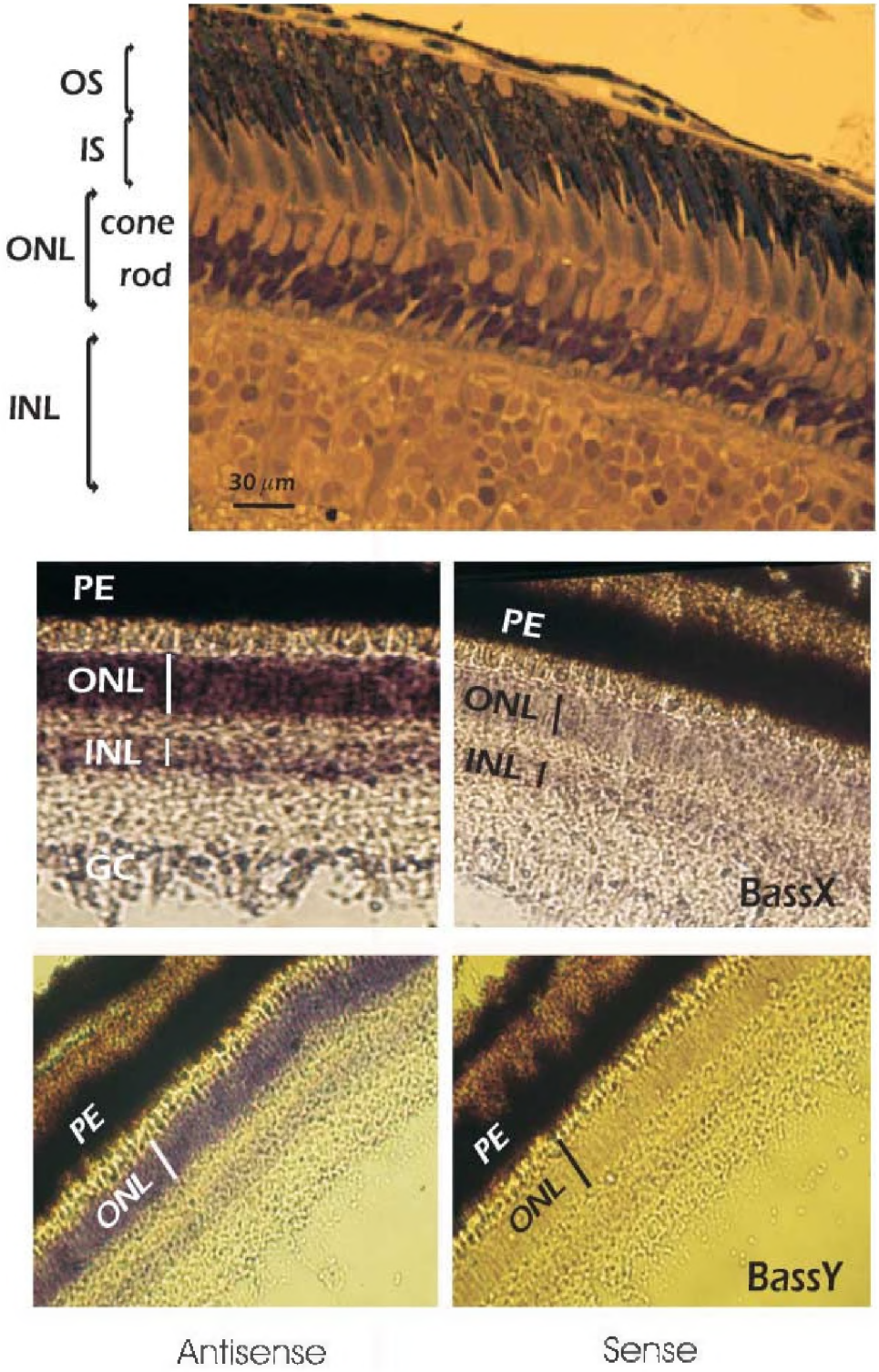

Fig. 1. *In-situ* hybridization with BassX and BassY RNA probes. The upper most panel is a micrograph of a thin section of light-adapted, fixed bass retina stained with toluidine blue. Pigment epithelium (PE) interdigitates the cone outer segments (OS) and embeds the rod outer segment. In the cone inner segment (IS), the myoid is fully contracted and the ellipsoid butts against the outer limiting membrane. The cone nuclei are located in the most distal layer of the outer nuclear layer (ONL) and can be distinguished as continuous with the cone inner segment. Rod nuclei are organized in 3–4 layers adjacent to the outer plexiform layer, which separates the inner nuclear layer (INL) from the ONL. The lower panels are micrographs of retinal frozen sections hybridized with antisense (left) and sense (right) digoxigenin-labeled RNA probes. Probe hybridization to cellular mRNA is evident by the purple-colored precipitate homogenously distributed through the ONL. Sense probes did not hybridize (absence of purple reaction product over the ONL), demonstrating the specificity of the molecular probe. At the stringency of hybridization tested (the highest compatible with tissue preservation), results demonstrates high level of BassX and BassY channel mRNA expression in the outer nuclear layer and the cone ellipsoid, but there is no distinction between rods and cones. BassX is also expressed at a low level in some cells of the INL (presumably bipolar cells (Henry et al., 2003)). BassY is only expressed in photoreceptors.

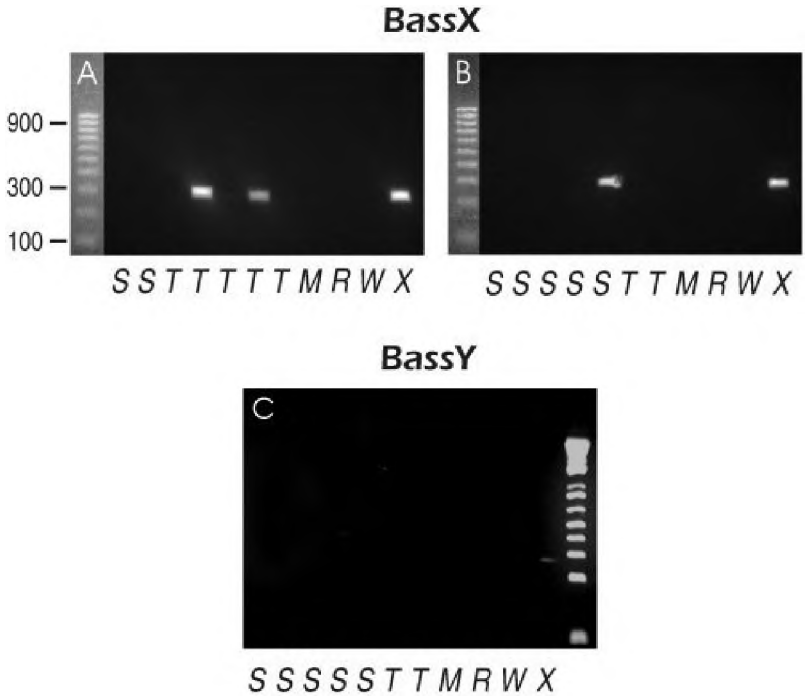

Fig. 2. Agarose gel electrophoresis of reaction products obtained by PCR amplification of single photoreceptor cDNA. Cellular reaction substrates were single cones (S) or twin cones (T). Negative controls were "sham" samples (M) consisting of cell bathing medium in the tissue chamber, distilled water (W), or Ringer's solution (R). Positive control was cRNA (30 fg) synthesized from the BassX cDNA clone (X). In Panels A and B are shown products of PCR reactions primed with BassX specific primers. The detection of products of the expected size and sequence proves this clone is the cone α subunit, sbCNGA3. In Panel C are shown products of PCR reactions primed by BassY specific primers in single and twin cones. The absence of reaction product demonstrates this clone is not expressed in cone photoreceptors. Size markers increment progressively between 100 and 1000 bp in 100-bp steps.

an ethidium-bromide-stained gel of PCR amplification product synthesized in individual cones using primers specific to the BassZ sequence. A single reaction product was detected in several single and twin cones, but not in every photoreceptor. The same product was detected using BassZ cDNA as substrate (lane Z), but not in "sham" samples (lane M). The reaction product was about 450 bp in size, just as predicted for the amplicon (457 bp). Nucleotide sequence of this single product was identical to the corresponding segment of BassZ. Thus, Bass Z is, indeed, the β subunit of the cone photoreceptors (sbCNGB3).

Single-cell immunocytochemistry

To confirm the cellular assignment of sbCNGA1 and sbCNGA3 and to develop necessary bio-tools, we produced polyclonal antibodies in rabbits injected with synthetic peptides. The synthetic peptides were designed based on two observations: (1) Wohlfart et al. (1992) have demonstrated that in bovine rod CNG α subunits, the extracellular loop between transmembrane segment 5 and the pore loop is antigenic. This antibody is the only one previously reported to bind the channel's extracellular surface. (2) The corresponding loops differ in sequence in sbCNGA1 (amino acids P282–P295) and sbCNGA3 (amino acids R303–R315).

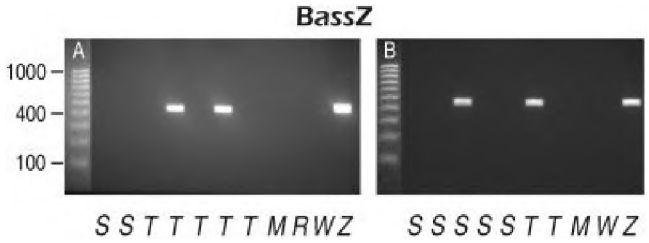

Fig. 3. Agarose gel electrophoresis of reaction products obtained by PCR amplification of individual photoreceptor cDNA. Cellular reaction substrates were single cones (S) or twin cones (T). Negative controls were "sham" samples (M) consisting of cell bathing medium in the tissue chamber, distilled water (W), or Ringer's solution (R). Positive control was the BassZ cDNA clone (Z). Detection of products of the expected size and sequence proves BassZ clone is cone specific. Size markers increment progressively between 100 and 1000 bp in 100-bp steps.

Microphotographs of unfixed, intact bass rods and cones labeled with antiRod or antiCone primary antibodies are shown in Fig. 4. Rods have small outer segments, typically 1.6 × 40 μm (diameter × length). Single cone outer segment dimensions are typically 5 × 15 μm (base diameter × length) with a tip diameter of about 3 μm. Twin cones are joined pairs of identical cells, each with typical outer segment dimensions 6 × 20 μm (base diameter × length) and 4 μm tip diameter. Antibody binding was revealed with fluorescent labeled anti-rabbit secondary antibodies. Fluorophores were either Cy3 or Alexa594 (red emitting) to minimize autofluorescence typical of photoreceptors. In Fig. 4 images acquired under bright-field illumination are shown side by side with those acquired under epifluorescent illumination. The rods labeled with antiRod antibody, but *did not* label with antiCone. On the other hand, both single and twin cones labeled with the antiCone antibody, but *not* with antiRod. The photoreceptor-specific antibodies labeled only the outer segment and the label appeared punctuate. The punctuate appearance of the fluorescent marker suggests that antibody labeling caused channel clustering or aggregation, since all evidence is that channels, at least in rods, are uniformly distributed over the membrane surface (electron microscopy: Cook et al., 1989; electrophysiology: Karpen et al., 1992). The results confirm that, indeed, the assignment of bass and cone CNG α subunits made from the PCR is correct and the same channel is expressed in single and twin cones. Moreover, we have produced antibodies that label the extracellular surface of the channels and recognize their epitope in intact cells.

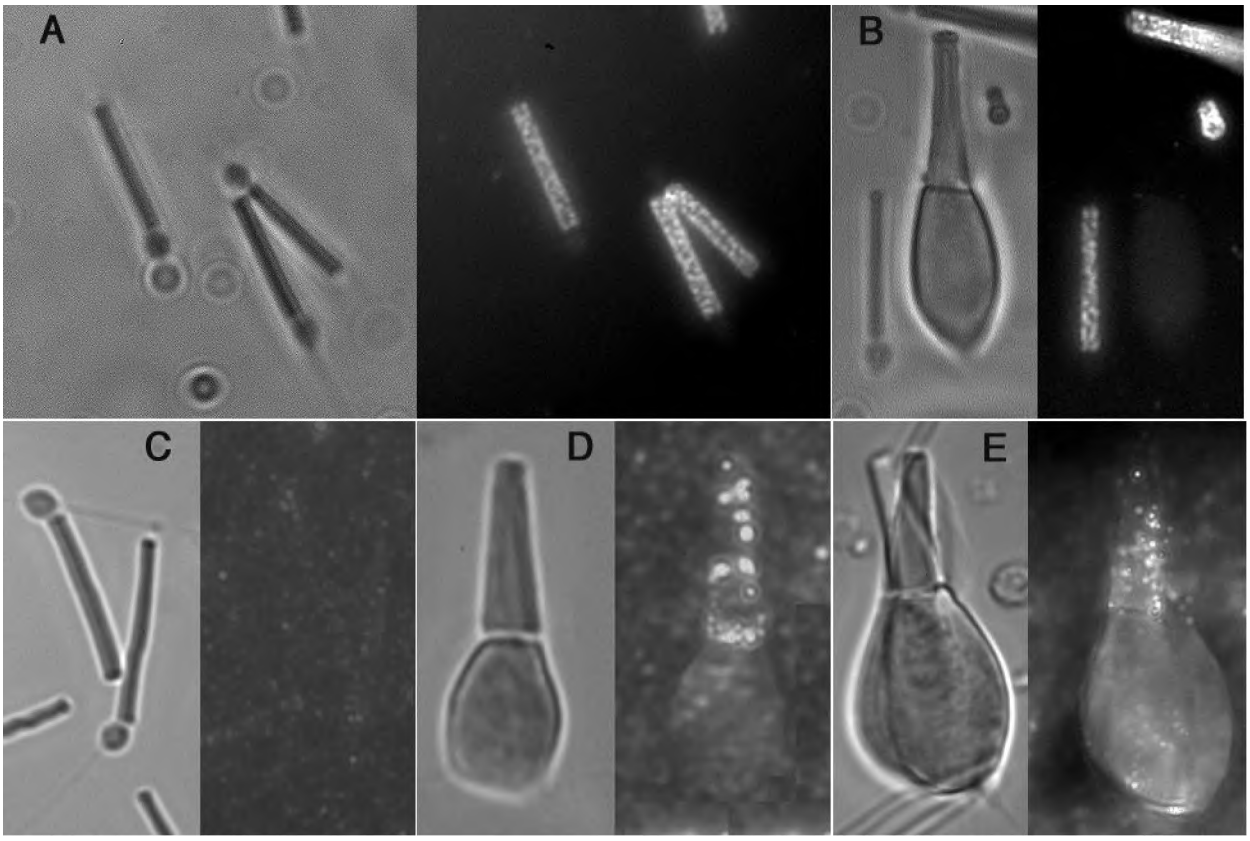

Fig. 4. Single-cell immunocytochemistry of unfixed, intact bass photoreceptors. The upper panels illustrate photoreceptors labeled with antiRod primary antibody and the lower ones cells labeled with antiCone primary antibody. Panels A and B are photoreceptors labeled with antiRod primary antibody. Shown are bright-field and epifluorescent images of the same field of isolated rod cells (A) or cone and rods (B). The rod outer segments are labeled, but the single cone is not. Panels C, D, and E are photoreceptors labeled with antiCone primary antibody. Shown are bright-field and epifluoresecent images of the same field of isolated rod cells (C), single (D), or twin (E) cones. AntiCone antibody does not bind to rods. Punctate label is observed in both single and twin cone outer segments, but not in their inner segment.

Molecular characterization of bass photoreceptor CNG channels

mRNA

We identified mRNA transcripts by high stringency hybridization of gene-specific probes to total retinal RNA blots. sbCNGA1 and sbCNGA3 were identified with RNA probes specific for the N-terminal region of the channel α subunits (the same as those used for *in-situ* hybridization). sbCNGB3 was identified with a DNA probe encoding amino acids A116 to V267.

Unlike the relatively low stringency conditions attainable under *in-situ* hybridization conditions, the high stringency conditions used in the analysis of RNA blots prevented cross hybridization between probes and nonspecific targets. The sbCNGA3 probe identified a single 3.4-kb transcript, consistent with the sbCNGA3 coding sequence (1956 bp) (Fig. 8). The sbCNGB3 probe identified a single 3.3-kb transcript, again reasonable for the sbCNGB3 coding sequence (2265 bp) (Fig. 8). The sbCNGA1 probe identified two transcripts, a prominent one of 2.9 kb and a less intense one of 1.8 kb (Fig. 8). Only the large mRNA species is consistent with the full-length coding sequence of sbCNGA1 (2040 bp). The 1.8-kb transcript may be an alternative spliced form of the transcribed gene.

Protein

Nucleotide sequences have been deposited in the GenBank database (http://www.ncbi.nih.gov). sbCNGA3, accession No. DQ172908; sbCNGB3, accession No. DQ172909; sbCNGA1, accession No. DQ172910. The deduced amino acid sequence of the bass rod CNG α subunit and cone CNG α and β subunits are presented in Figs. 5–7. The bass CNG sequences are aligned and compared with those in human and mouse, the only other species in which all the matching channels have also been cloned. The features common to all known CNG channels are identified: six transmembrane helices (S1–S6), voltage sensor motif in S4, pore loop between S5 and S6, cyclic nucleotide binding domain (CNBD) and the C-linker between the CNBD and helix 6.

We determined the apparent molecular mass of rod and cone α subunits in the retina by SDS-PAGE under reducing conditions. The open reading frame of sbCNGA1 encodes 679 amino acid residues with a calculated molecular mass of $\approx$79.5 kDa. Immunoblotting of striped bass retinal homogenate indicates the apparent mobility of the authentic protein is 96 kDa (Fig. 9). sbCNGA3 encodes a polypeptide 651 amino acid long with a calculated molecular mass of $\approx$75.5 kDa. The authentic protein in the western blots has an apparent molecular mass of 74 kDa (Fig. 9). sbCNGB3 encodes a 754 amino acid residues protein with a calculated

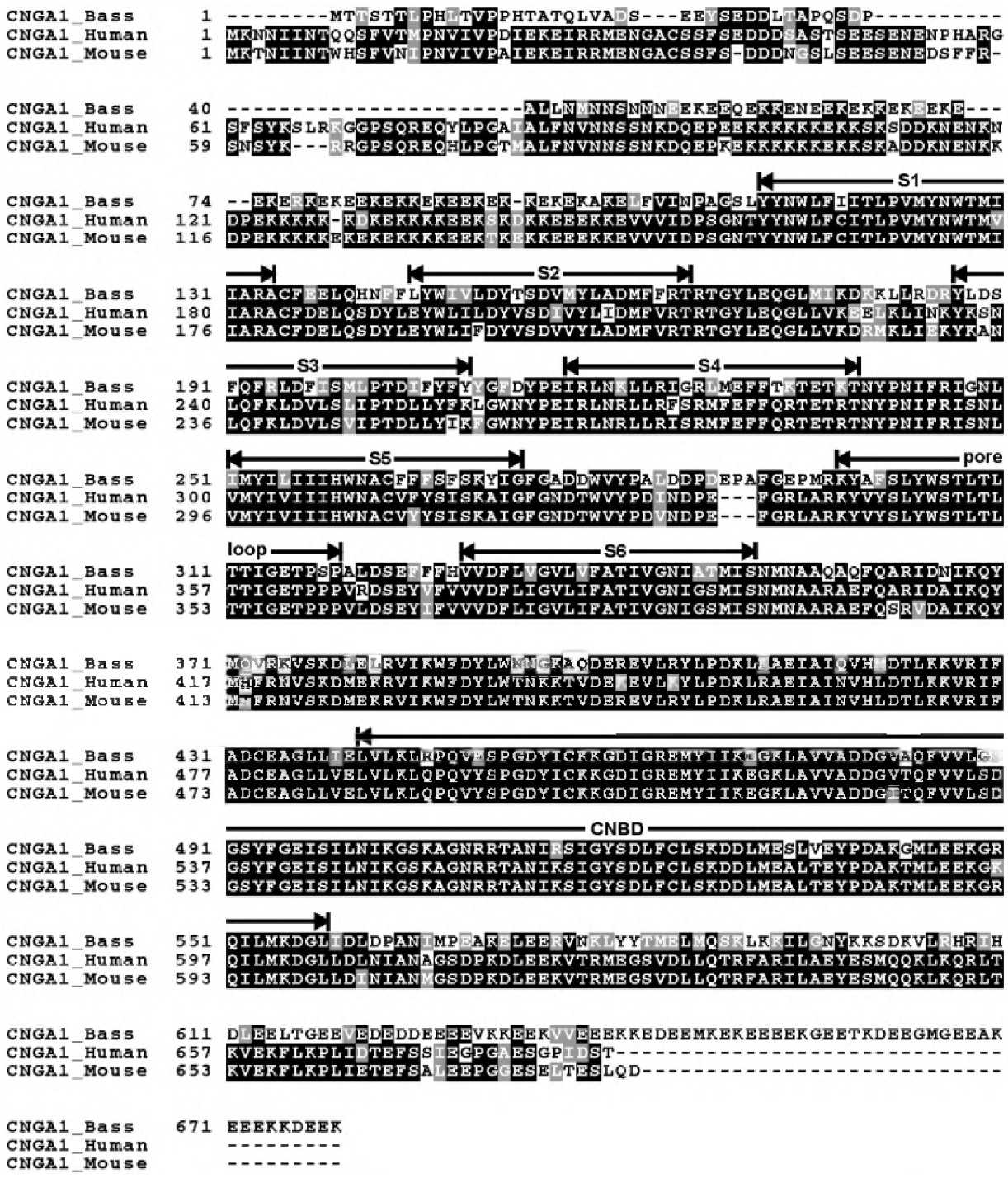

Fig. 5. Deduced amino acid sequence of bass rod α subunit (sbCNGA1) aligned with corresponding subunits in human and mouse photoreceptors. Identical amino acids are identified in black box shades and conservative homologues in gray box shades.

molecular mass of ≈85.1 kDa. We were unable to determine sbCNGB3 protein apparent molecular mass because we lack specific antibodies.

Discussion

We cloned the α and β subunits of the CNG ion channel of striped bass cones and the α subunit of the channels in rods. Although cone subtypes can be recognized by their cell architecture, visual pigment identity and physiological response to light they all express the same channel protein. Single-cell RT-PCR and single-cell immunocytochemistry with monospecific antibodies allowed the unambiguous determination of the cell of origin of the channels we have cloned. Because single photoreceptors were collected following retinal shredding, particular technical care was necessary to minimize "false positives" caused by damaged cells expelling

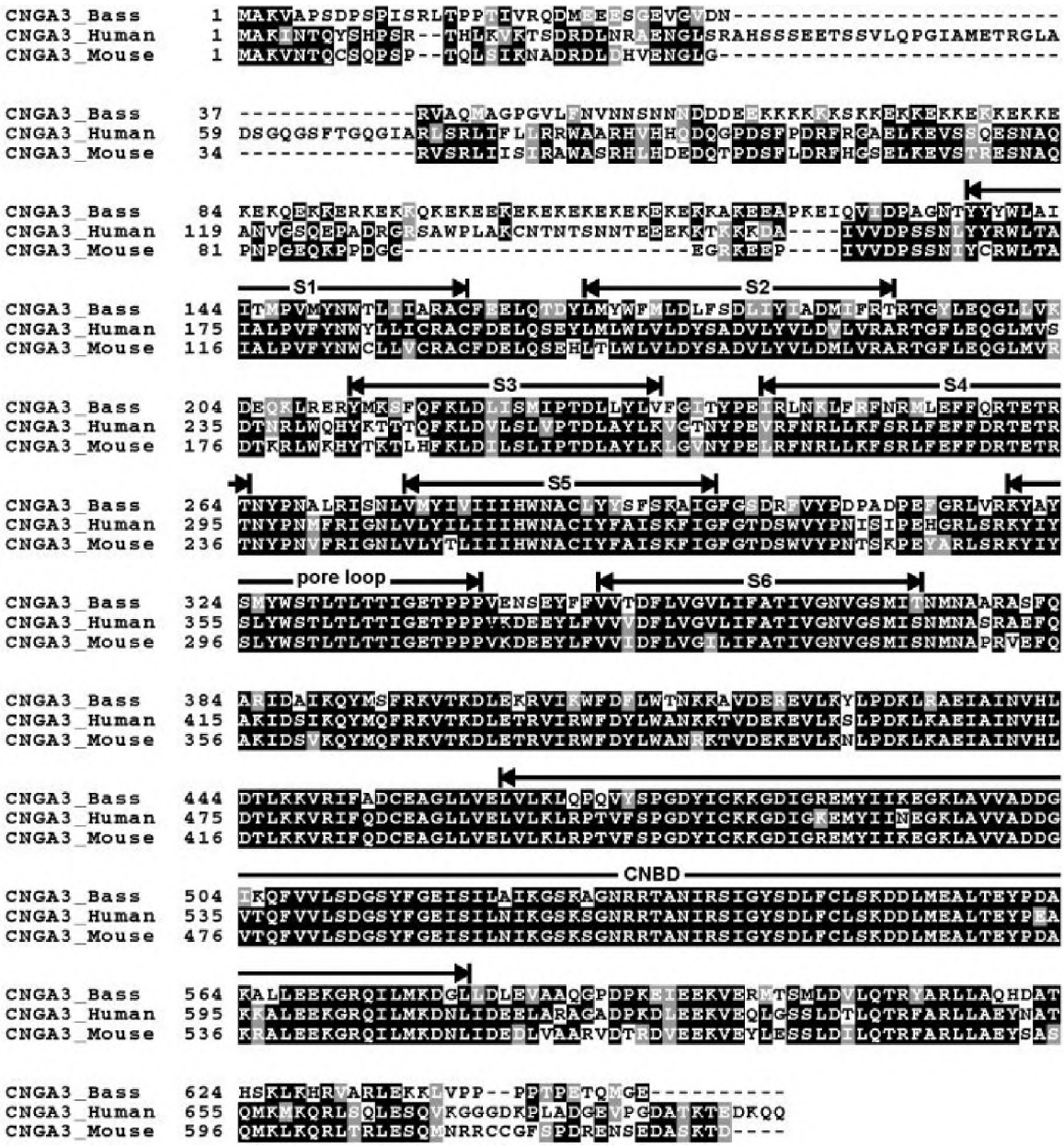

Fig. 6. Deduced amino acid sequence of bass cone α subunit (sbCNGA3) aligned with corresponding subunits in human and mouse photoreceptors. Where amino acids are identical, a black box shade is used. Conservative amino acid substitutions are indicated with a gray shade box. Structural domains common to all CNG ion channels are indicated by horizontal lines: six transmembrane helices (S1–S6), pore loop (P), and cyclic nucleotide binding domain (CNBD).

genomic DNA into the bathing medium. In goldfish, bipolar cells express CNG channel α subunits identical to those in cones (Henry et al., 2003). There is no reason to doubt the same is true in striped bass; however, our *in-situ* hybridization data indicate, not surprisingly, that expression levels of the channel in bipolar cells is much lower than in the photoreceptors and that not all bipolar cell subtypes may express the channel.

Phylogenetic comparison

An interesting follow up to the accumulation of sequences of a given protein in the same cell type across species is a phylogenetic analysis to infer evolutionary relationships amongst the cells (Felsenstein, 2004). For example, phylogenetic analysis of visual pigments (VP) suggests particular pathways for the adaptive evolution of color vision in vertebrates (reviewed by Yokoyama, 2002; Collin & Trezise, 2004). A general problem in creating phylogenetic trees is that several trees are plausible, and even optimization may not yield the very best possibility. To arrive at an optimum channel phylogenetic tree, we optimized possible choices through the iterative application of three tree algorithms: Fitch, Kitsch and Nearest Neighbor in PHYLIP v. 3.63 (Phylogeny Inference Package). The Kitsch tree (Fig. 10) was the optimum heuristic model and it was identical when scrutinized with several

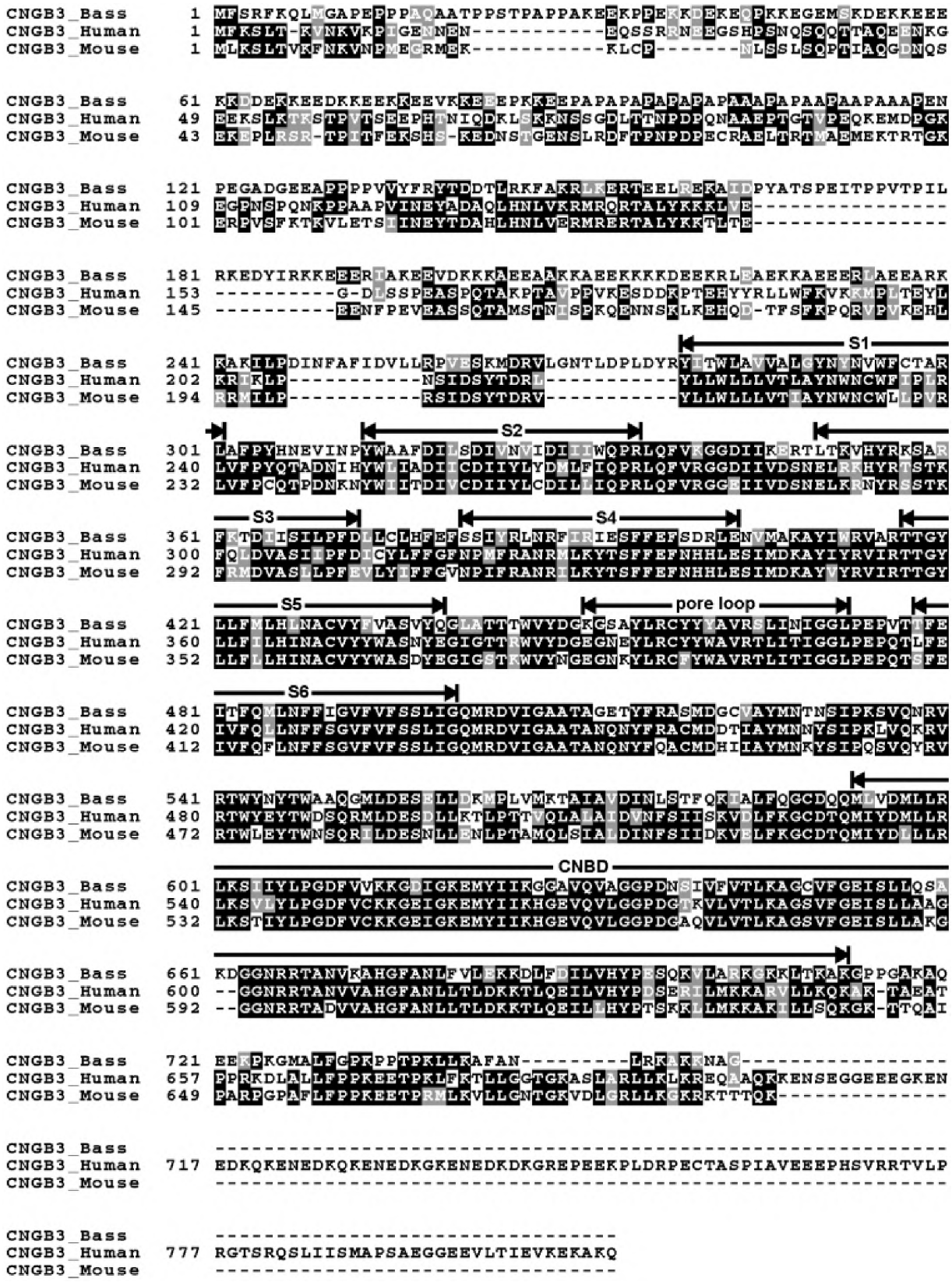

Fig. 7. Deduced amino acid sequence of bass cone β subunit (sbCNGB3) aligned with corresponding subunits in human and mouse photoreceptors. Identical amino acids are identified in black box shades and conservative homologues in gray box shades.

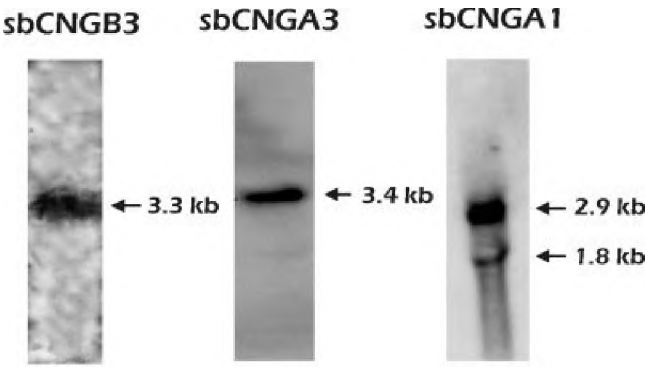

Fig. 8. Retinal RNA blot. Specific bass CNGB3, CNGA3, and CNGA1 mRNA were identified in blots by high stringency hybridization to nucleic acid probes. As labeled in the figure, RNA transcript for CNGB3 is 3.3 kb, CNGA3 is 3.4 kb, and for CNGA1 they are 1.8 and 2.9 kb in size.

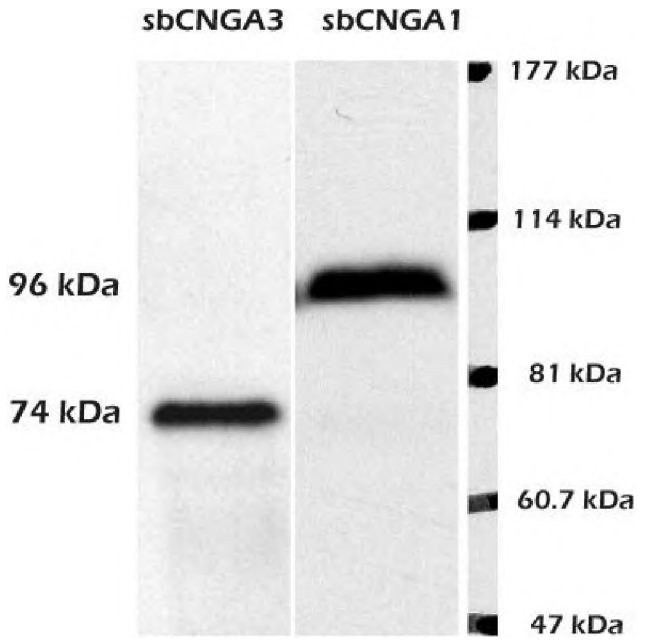

Fig. 9. Retinal protein blot. Specific CNGA1 and CNGA3 proteins were identified in protein blots by binding of specific primary antibodies. The apparent mobility of the CNGA1 α protein is 96 kDa, while that of CNGA3 is 76 kDa. The relative mobility of polypeptide mass standards (Bench marker, Invitrogen) run alongside each protein sample in SDS-PAGE is indicated.

theoretical models [Jones-Taylor-Thornton, PAM, Kimura and Category similarity, Felsenstein (2004)]. The tree reflects early divergence between vertebrate and invertebrate channels. The CNG phylogenetic map is entirely consistent with conclusions reached from analysis of VP trees. Rod and cone channels arise from a common progenitor, but they constitute distinct and robust branches in the tree. The cone branch is defined earlier in evolution than the rod one. In the cone branch, distinct lines exist for fish, birds, and mammals. Fish and bird channels are specified at about the same time, and significantly ahead of mammals. Unlike VP, however, there is only one molecular class of cone channels. Rod channels in mammals are the most recently evolved of the α subunits. Bass photoreceptor CNG ion channels, like all CNG channels, are constituted by six transmembrane helices, a pore loop, a cytoplasmic CNBD and a C-linker between S5 and the CNBD (Figs. 4–6). We compare bass photoreceptor channels to other CNG channels in structural details that relate to their function.

Ca^{2+} selectivity and voltage-dependent block

In both rod and cone CNG channels Ca^{2+} ions both permeate through and bind to the pore assembled by the heteromeric complex of four pore loops. As a consequence, Ca^{2+} is both a significant carrier of the current through open channels and a voltage-dependent blocker (rods: Zimmerman & Baylor, 1992; Colamartino et al., 1991; Tanaka & Furman, 1993; cones: Picones & Korenbrot, 1995; Haynes, 1995*a*). These biophysical features are quantitatively explained by a model that assumes Ca^{2+} binds to two distinct sites within the pore (rods: Wells & Tanaka, 1997; cones: Ohyama et al., 2002). A glutamate residue near the pore's extracellular opening (E363 in bovine CNGA1) is a critical constituent of the externally accessible Ca^{2+}-binding site (Root & MacKinnon, 1993; Eismann et al., 1994). This critical glutamate and its neighbor residues are absolutely conserved in all CNG α subunits, including bass (E315 in sbCNGA1 and E337 in sbCNGA3) but not in the non-ion-conductive β subunits. The channel Ca^{2+} binding and selectivity features, however, are profoundly different in rods and cones (Picones & Korenbrot, 1995*a*; Frings et al., 1995; Ohyama et al., 2000). In mammalian channels, Ca^{2+} binding is regulated by the pore flanking transmembrane helices S5 and S6 which control the protonation state of pore glutamates (Seifert et al., 1999). The structural features within S5 and S6 that control protonation, however, are global and there is not a single locus whose mutation explains the control of selectivity (Seifert et al., 1999). The sequence of S5 and S6 in bass rod and cone channels is, indeed, not identical and amino acid differences are generally not conservative (Figs. 4 and 5). Exploration of the functional consequence of these structural differences will help elucidate the molecular mechanisms of Ca^{2+} binding and permeation.

S4 domain

All CNG channels share a structural motif in the fourth transmembrane helix, referred to as "S4," consisting of (+)xx(+)xx (+)xx(+)xx, where (+) is positively charged Arg or Lys. The surprising presence of charged residues within the transmembrane helix is common to all voltage-gated channels and the residues act as membrane voltage sensors (reviewed by Bezanilla, 2000). CNG channels are not voltage-gated, yet S4 is well conserved because this motif plays a critical role in the intracellular channel protein processing and transport (Faillace et al., 2004). The S4 domain is preserved in bass rod (R218–M229) and cone (R243–L254) α subunits. Interestingly, the basic S4 motif is also expressed in the β subunit bass CNGB3 (R385–E393), but it consists of only 3 (+)xx repeats, the shortest possible repeat found in all of the members of the extended gene family, including voltage-gated K^+ and HCN channels.

Phosphorylation

Rod CNG channels can be phosphorylated by tyrosine kinase. Phosphorylation of tyrosine Tyr498 in the bovine CNGA1 subunit and Tyr1097 in the bovine CNGB1 subunit decreases the apparent affinity for cGMP and interferes with a Ca^{2+}-calmodulin-dependent

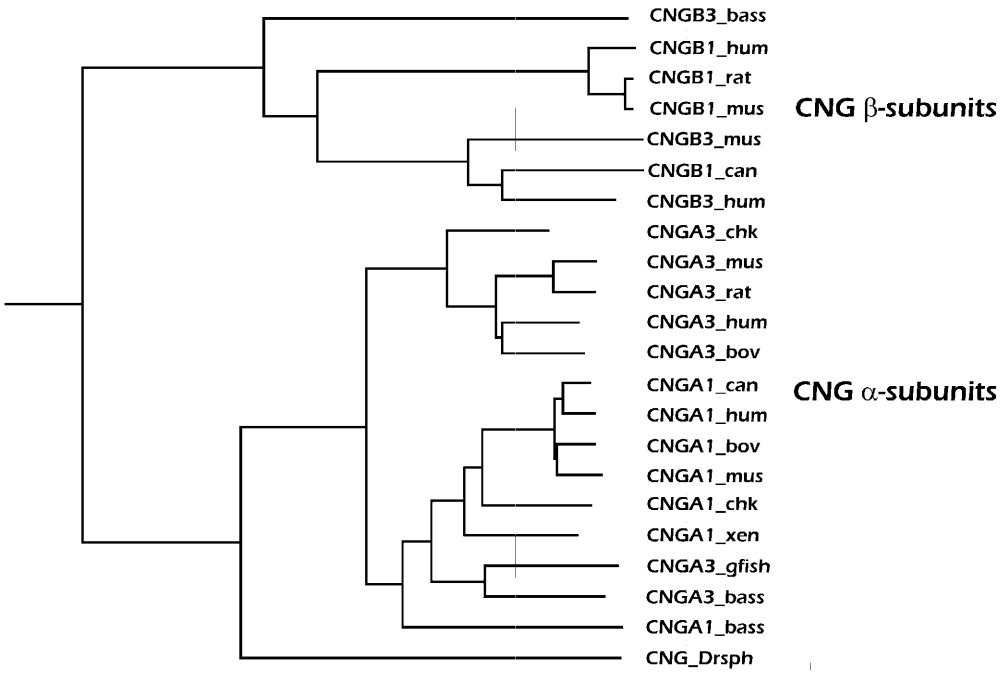

Fig. 10. Phylogenetic tree depicts the evolutionary relationship amongst rod and cone CNG α and β subunit genes. The length of the horizontal bars is a measure of distance in time from a moment of evolutionary divergence.

regulation of cGMP sensitivity (Molokanova et al., 1999, 2003; Krajewski et al., 2003). The state of channel phosphorylation in intact cells and whether it changes in the course of phototransduction is unknown, however, insulin-like growth factor-1 causes dephosphorylation of the crucial tyrosine residues (Molokanova et al., 2003). In bovine CNGA1, Tyr498 is within the CNBD, a comparably located residue exists in sbCNGA1, Tyr493 and sbCNGA3, Tyr489. In bovine CNGA3 phosphorylation of residues Ser577 and Ser579 changes the channels' sensitivity to cGMP (Muller et al., 2001). Corresponding residues in sbCNGA3 could be Ser527 and Ser529.

N-linked glycosylation

N-linked glycosylation is a common posttranslational modification frequently necessary to guide and target intracellular transport of channel proteins that requires the consensus sequence Nx(S,T) (reviewed by Deutsch, 2003). Every mammalian rod and cone CNG channels have an Asn residue in the extracellular loop between S5 and the pore and this residue is acetyl-glycosylated (Wohlfart et al., 1989; Faillace et al., 2004). Notably, the corresponding extracellular loop in bass rod α and cone α subunits entirely lacks Asn (sbCNGA1 residues F274 to M296; sbCNGA3 residues F299 to R319). The residue best aligned with Asn in both rod and cone channels is Asp and, moreover, Asn is not present at all on the extracellular surface of the bass channels. It would appear that these channels are not N-acetyl glycosylated and that channel protein intracellular processing is different in fish than in mammals. In this context, we note that both rod and cone bass cDNA clones failed to yield functional channels when expressed in mammalian HEK293 cells under the CMV promoter, a construct that efficiently promotes expression of rod and cone bovine channel cDNA (Faillace et al., 2004). Heterologous expression in fish derived cultured cells is yet to be explored.

Modulation by calmodulin (CaM)

In mammalian rod channels, Ca^{2+}/CaM binds with high affinity to the cytoplasmic N-terminus of the CNGB1 subunit and weakens an intramolecular interaction between the N- and C-termini of the CNGB1 and CNGA1 channel subunits (Trudeau & Zagotta, 2003, 2004). This mechanism helps explain the Ca^{2+}/CaM-dependent modulation of cGMP sensitivity in rod channels in the native membrane (Hsu & Molday, 1994). In contrast, native cone channels are not modulated by CaM (Hackos & Korenbrot, 1997; Haynes & Stotz, 1997), although physiologically significant Ca^{2+}-dependent modulation of ligand sensitivity occurs in cones through the action of a soluble factor, yet to be identified (Rebrik et al., 2000; Rebrik & Korenbrot, 2004). Cloned human cone channels in heterologous expression systems, nonetheless, exhibit small changes in ligand sensitivity in the presence and absence of Ca^{2+}/CaM (Peng et al., 2003). This modulation depends on CaM-binding domains in the channel β subunit (sequence L132 to K147), but not in α. We used the CaM-binding consensus sequence in humans to search a comparable sequence in bass CNGB3. While several alignment algorithms converged on the same, unique sequence match (amino acids L143 to R158), the identity of the sequences was only 41% (Smith-Waterman function), not a reliable match. The inability of exogenous CaM to modulate cone CNG channels, the ineffectiveness on cone channel modulation of drugs that interfere with CaM, and the lack of distinctive CaM binding sequences reinforce the thesis that cone channel modulation is not mediated by CaM. The cloned channels should be of help in discovering the modulator.

Acknowledgments

We thank K. Bailey and A. Faynboym for their dedicated technical effort and C. Chung and S. Durdan for their valuable comments on the manu-

script. This research supported by NIH grant EY-05498 and The Sandler Fund at UCSF.

References

Ahmad, I., Leinders-Zufall, T., Kocsis, J.D., Shepherd, G.M., Zufall, F. & Barnstable, C.J. (1994). Retinal ganglion cells express a cGMP-gated cation conductance activatable by nitric oxide donors. *Neuron* **12**, 155–165.

Ausubel, F.M., Brent, R., Kingston, R.E., Moore, D.D., Seidman, J.G., Smith, J.A. & Struhl, K. (2005). *Current Protocols in Molecular Biology*. New York: Greene Publishing Associates and Wiley-Interscience.

Barry, P.H. (2003). The relative contributions of cAMP and InsP3 pathways to olfactory responses in vertebrate olfactory receptor neurons and the specificity of odorants for both pathways. *Journal of General Physiology* **122**, 247–250.

Bezanilla, F. (2000). The voltage sensor in voltage-dependent ion channels. *Physiological Reviews* **80**, 555–92.

Biel, M., Seeliger, M., Pfeifer, A., Kohler, K., Gerstner, A., Ludwig, A., Jaissle, G., Fauser, S., Zrenner, E. & Hofmann, F. (1999). Selective loss of cone function in mice lacking the cyclic nucleotide-gated channel CNG3. *Proceedings of the National Academy of Sciences of the U.S.A.* **96**, 7553–7557.

Chen, T.Y., Peng, Y.W., Dhallan, R.S., Ahamed, B., Reed, R.R. & Yau, K.W. (1993). A new subunit of the cyclic nucleotide-gated cation channel in retinal rods. *Nature* **362**, 764–767.

Chomczynski, P. & Sacchi, N. (1987). Single-step method of RNA isolation by acid guanidinium thiocyanate-phenol-chloroform extraction. *Analytical Biochemistry* **162**, 156–159.

Colamartino, G., Menini, A. & Torre, V. (1991). Blockage and permeation of divalent cations through the cyclic GMP-activated channel from tiger salamander retinal rods. *Journal of Physiology* **440**, 189–206.

Collin, S.P. & Trezise, A.E. (2004). The origins of colour vision in vertebrates. *Clinical and Experimental Optometry* **87**, 217–223.

Cook, N.J., Hanke, W. & Kaupp, U.B. (1987). Identification, purification, and functional reconstitution of the cyclic GMP-dependent channel from rod photoreceptors. *Proceedings of the National Academy of Sciences of the U.S.A.* **84**, 585–589.

Cook, N.J., Molday, L.L., Reid, D., Kaupp, U.B. & Molday, R.S. (1989). The cGMP-gated channel of bovine rod photoreceptors is localized exclusively in the plasma membrane. *Journal of Biological Chemistry* **264**, 6996–6999.

Deutsch, C. (2003). The birth of a channel. *Neuron* **40**, 265–276.

Ebrey, T. & Koutalos, Y. (2001). Vertebrate photoreceptors. *Progress in Retinal Eye Research* **20**, 49–94.

Eismann, E., Muller, F., Heinemann, S.H. & Kaupp, U.B. (1994). A single negative charge within the pore region of a cGMP-gated channel controls rectification, Ca^{2+} blockage, and ionic selectivity. *Proceedings of the National Academy of Sciences of the U.S.A.* **91**, 1109–1113.

Failace, M.P., Bernabeu, R.O. & Korenbrot, J.I. (2004). Cellular processing of cone photoreceptor cyclic GMP-gated ion channels: A role for the S4 structural motif. *Journal of Biological Chemistry* **279**, 22643–22653.

Felsenstein, J. (2004). *Inferring Phylogenetics*. Sunderland, Massachusetts: Sinauer Associates.

Frings, S., Seifert, R., Godde, M. & Kaupp, U.B. (1995). Profoundly different calcium permeation and blockage determine the specific function of distinct cyclic nucleotide-gated channels. *Neuron* **15**, 169–179.

Gerstner, A., Zong, X., Hofmann, F. & Biel, M. (2000). Molecular cloning and functional characterization of a new modulatory cyclic nucleotide-gated channel subunit from mouse retina. *Journal of Neuroscience* **20**, 1324–1332.

Hackos, D.H. & Korenbrot, J.I. (1997). Calcium modulation of ligand affinity in the cyclic GMP-gated ion channels of cone photoreceptors. *Journal of General Physiology* **110**, 515–528.

Hackos, D.H. & Korenbrot, J.I. (1999). Divalent cation selectivity is a function of gating in native and recombinant cyclic nucleotide-gated ion channels from retinal photoreceptors. *Journal of General Physiology* **113**, 799–818.

Haynes, L.W. (1995). Permeation and block by internal and external divalent cations of the catfish cone photoreceptor cGMP-gated channel. *Journal of General Physiology* **106**, 507–523.

Haynes, L.W. & Stotz, S.C. (1997). Modulation of rod, but not cone, cGMP-gated photoreceptor channel by calcium-calmodulin. *Visual Neuroscience* **14**, 233–239.

Henry, D., Burke, S., Shishido, E. & Matthews, G. (2003). Retinal bipolar neurons express the cyclic nucleotide-gated channel of cone photoreceptors. *Journal of Neurophysiology* **89**, 754–761.

Hofmann, F., Biel, M. & Kaupp, U.B. (2003). International Union of Pharmacology. XLII. Compendium of voltage-gated ion channels: Cyclic nucleotide-modulated channels. *Pharmacological Review* **55**, 587–589.

Hsu, Y.T. & Molday, R.S. (1994). Interaction of calmodulin with the cyclic GMP-gated channel of rod photoreceptor cells. Modulation of activity, affinity purification, and localization. *Journal of Biological Chemistry* **269**, 29765–29770.

Hutti, S., Michalakis, S., Seeliger, M., Luo, D.G., Acar, N., Geiger, H., Hudl, K., Mader, R., Haverkamp, S., Moser, M., Pfeifer, A., Gerstner, A., Yau, K.W. & Biel, M. (2005). Impaired channel targeting and retinal degeneration in mice lacking the cyclic nucleotide-gated channel subunit CNGB1. *Journal of Neuroscience* **25**, 130–138.

Ivics, Z., Kaufman, C.D., Zayed, H., Miskey, C., Walisko, O. & Izsvak, Z. (2004). The Sleeping Beauty transposable element: Evolution, regulation and genetic applications. *Current Issues in Molecular Biology* **6**, 43–55.

Karpen, J.W., Loney, D.A. & Baylor, D.A. (1992). Cyclic GMP-activated channels of salamander retinal rods: Spatial distribution and variation of responsiveness. *Journal Of Physiology* **448**, 257–274.

Kaupp, U.B., Niidome, T., Tanabe, T., Terada, S., Bonigk, W., Stuhmer, W., Cook, N.J., Kangawa, K., Matsuo, H., Hirose, T., Miyata, T. & Numa, S. (1989). Primary structure and functional expression from complementary DNA of the rod photoreceptor cyclic GMP-gated channel. *Nature* **342**, 762–766.

Kaupp, U.B. & Seifert, R. (2001). Molecular diversity of pacemaker ion channels. *Annual Review of Physiology* **63**, 235–257.

Kaupp, U.B. & Seifert, R. (2002). Cyclic nucleotide-gated ion channels. *Physiological Reviews* **82**, 769–824.

Korenbrot, J.I. & Rebrik, T.I. (2002). Tuning outer segment Ca^{2+} homeostasis to phototransduction in rods and cones. *Advances Experimental Medical Biology* **514**, 179–203.

Korschen, H.G., Illing, M., Seifert, R., Sesti, F., Williams, A., Gotzes, S., Colville, C., Muller, F., Dose, A., Godde, M., Molday, L., Kaupp, U.B. & Molday, R.S. (1995). A 240 kDa protein represents the complete β subunit of the cyclic nucleotide-gated channel from rod photoreceptors. *Neuron* **15**, 627–636.

Krajewski, J.L., Luetje, C.W. & Kramer, R.H. (2003). Tyrosine phosphorylation of rod cyclic nucleotide-gated channels switches off Ca^{2+}/calmodulin inhibition. *Journal of Neuroscience* **23**, 10100–10106.

Leconte, L. & Barnstable, C.J. (2000). Impairment of rod cGMP-gated channel α-subunit expression leads to photoreceptor and bipolar cell degeneration. *Investigative Ophthalmology and Visual Science* **41**, 917–926.

Lee, H.M., Park, Y.S., Kim, W. & Park, C.S. (2001). Electrophysiological characteristics of rat gustatory cyclic nucleotide—gated channel expressed in Xenopus oocytes. *Journal of Neurophysiology* **85**, 2335–2349.

Matulef, K. & Zagotta, W.N. (2003). Cyclic nucleotide-gated ion channels. *Annual Review Cell Developmental Biology* **19**, 23–44.

Miller, J.L. & Korenbrot, J.I. (1993). Phototransduction and adaptation in rods, single cones, and twin cones of the striped bass retina: A comparative study. *Visual Neuroscience* **10**, 653–667.

Misaka, T., Kusakabe, Y., Emori, Y., Gonoi, T., Arai, S. & Abe, K. (1997). Taste buds have a cyclic nucleotide-activated channel, CNG-gust. *Journal of Biological Chemistry* **272**, 22623–22629.

Molokanova, E., Krajewski, J.L., Satpaev, D., Luetje, C.W. & Kramer, R.H. (2003). Subunit contributions to phosphorylation-dependent modulation of bovine rod cyclic nucleotide-gated channels. *Journal of Physiology* **552**, 345–356.

Molokanova, E., Savchenko, A. & Kramer, R.H. (1999). Noncatalytic inhibition of cyclic nucleotide-gated channels by tyrosine kinase induced by genistein. *Journal of General Physiology* **113**, 45–56.

Muller, F., Vantler, M., Weitz, D., Eismann, E., Zoche, M., Koch, K.W.& Kaupp, U.B. (2001). Ligand sensitivity of the 2 subunit from the bovine cone cGMP-gated channel is modulated by protein kinase C but not by calmodulin. *Journal of Physiology* **532**, 399–409.

Nakatani, K., Koutalos, Y. & Yau, K.-W. (1995). Ca^{+} modulation of the cGMP-gated channel of bullfrog retinal rod photoreceptor. *Journal of Physiology* **484**, 69–76.

Ohyama, T., Hackos, D.H., Frings, S., Hagen, V., Kaupp, U.B. & Korenbrot, J.I. (2000). Fraction of the dark current carried by Ca(2+) through cGMP-gated ion channels of intact rod and cone photoreceptors. *Journal of General Physiology* **116**, 735–754.

Ohyama, T., Picones, A. & Korenbrot, J.I. (2002). Voltage-dependence of ion permeation in cyclic GMP-gated ion channels is optimized for cell function in rod and cone photoreceptors. *Journal of General Physiology* **119**, 341–354.

Peng, C., Rich, E.D., Thor, C.A. & Varnum, M.D. (2003). Functionally important calmodulin-binding sites in both NH_2- and COOH- terminal regions of the cone photoreceptor cyclic nucleotide-gated channel CNGB3 subunit. *Journal of Biological Chemistry* **278**, 24617–24623.

Peng, C., Rich, E.D. & Varnum, M.D. (2004). Subunit configuration of heteromeric cone cyclic nucleotide-gated channels. *Neuron* **42**, 401–410.

Picones, A. & Korenbrot, J.I. (1992). Permeation and interaction of monovalent cations with the cGMP-gated channel of cone photoreceptors. *Journal of General Physiology* **100**, 647–673.

Picones, A. & Korenbrot, J.I. (1995*a*). Permeability and interaction of Ca^{2+} with cGMP-gated ion channels differ in retinal rod and cone photoreceptors. *Biophysical Journal* **69**, 120–127.

Picones, A. & Korenbrot, J.I. (1995*b*). Spontaneous, ligand-independent activity of the cGMP-gated ion channels in cone photoreceptors of fish. *Journal of Physiology* **485**, 699–714.

Pugh, E.N., Jr. & Lamb, T.D. (2000). Phototransduction in vertebrate rods and cones: molecular mechanisms of amplification, recovery and light adaptation. In *Handbook of Biological Physics*, ed. Stavenga, D.G., DeGrip, W.J. & Pugh, E.N., Jr., pp. 186–255. Amsterdam: Elsevier Science B.V.

Raymond, P.A., Barthel, L.K., Rounsifer, M.E., Sullivan, S.A. & Knight, J.K. (1993). Expression of rod and cone visual pigments in goldfish and zebrafish: A rhodopsin-like gene is expressed in cones. *Neuron* **10**, 1161–1174.

Rebrik, T.I. & Korenbrot, J.I. (1998). In intact cone photoreceptors, a Ca^{2+}-dependent, diffusible factor modulates the cGMP-gated ion channels differently than in rods. *Journal of General Physiology* **112**, 537–548.

Rebrik, T.I. & Korenbrot, J.I. (2004). In intact mammalian photoreceptors, Ca^{2+}-dependent modulation of cGMP-gated ion channels is detectable in cones but not in rods. *Journal of General Physiology* **123**, 63–76.

Rebrik, T.I., Kotelnikova, E.A. & Korenbrot, J.I. (2000). Time course and Ca(2+) dependence of sensitivity modulation in cyclic GMP-gated currents of intact cone photoreceptors. *Journal of General Physiology* **116**, 521–534.

Root, M.J. & Mackinnon, R. (1993). Identification of an external divalent cation-binding site in the pore of a cGMP-activated channel. *Neuron* **11**, 459–466.

Sagoo, M.S. & Lagnado, L. (1996). The action of cytoplasmic calcium on the cGMP-activated channel in salamander rod photoreceptors. *Journal of Physiology* **497**, 309–319.

Seifert, R., Eismann, E., Ludwig, J., Baumann, A. & Kaupp, U.B. (1999). Molecular determinants of a Ca^{2+}-binding site in the pore of cyclic nucleotide-gated channels: S5/S6 segments control affinity of intrapore glutamates. *EMBO Journal* **18**, 119–130.

Subramaniam, S. (1998). The biology workbench—a seamless database and analysis environment for the biologist. *Protein* **32**, 1–2.

Sugita, M., Ohishi, H., Iwasa, Y., Hirono, C. & Shiba, Y. (2004). Extracellular proton sensing of the rat gustatory cyclic nucleotide-gated channel. *Biochemical Biophysical Research Communication* **319**, 369–374.

Tanaka, J.C. & Furman, R.E. (1993). Divalent effects on cGMP-activated currents in excised patches from amphibian photoreceptors. *Journal of Membrane Biology* **131**, 245–256.

Trudeau, M.C. & Zagotta, W.N. (2003). Calcium/calmodulin modulation of olfactory and rod cyclic nucleotide-gated ion channels. *Journal of Biological Chemistry* **278**, 18705–18708.

Trudeau, M.C. & Zagotta, W.N. (2004). Dynamics of Ca^{2+}-calmodulin-dependent inhibition of rod cyclic nucleotide-gated channels measured by patch-clamp fluorometry. *Journal of General Physiology* **124**, 211–223.

Weitz, D., Ficek, N., Kremmer, E., Bauer, P.J. & Kaupp, U.B. (2002). Subunit stoichiometry of the CNG channel of rod photoreceptors. *Neuron* **36**, 881–889.

Wells, G.B. & Tanaka, J.C. (1997). Ion selectivity predictions from a two-site permeation model for the cyclic nucleotide-gated channel of retinal rod cells. *Biophysical Journal* **72**, 127–140.

Wohlfart, P., Haase, W., Molday, R.S. & Cook, N.J. (1992). Antibodies against synthetic peptides used to determine the topology and site of glycosylation of the cGMP-gated channel from bovine rod photoreceptors. *Journal of Biological Chemistry* **267**, 644–648.

Wohlfart, P., Muller, H. & Cook, N.J. (1989). Lectin binding and enzymatic deglycosylation of the cGMP-gated channel from bovine rod photoreceptors. *Journal of Biological Chemistry* **264**, 20934–20939.

Yokoyama, S. (2002). Molecular evolution of color vision in vertebrates. *Gene* **300**, 69–78.

Zagotta, W.N. & Siegelbaum, S.A. (1996). Structure and function of cyclic nucleotide-gated channels. *Annual Review of Neuroscience* **19**, 235–263.

Zheng, J., Trudeau, M.C. & Zagotta, W.N. (2002). Rod cyclic nucleotide-gated channels have a stoichiometry of three CNGA1 subunits and one CNGB1 subunit. *Neuron* **36**, 891–896.

Zhong, H., Molday, L.L., Molday, R.S. & Yau, K.W. (2002). The heteromeric cyclic nucleotide-gated channel adopts a 3A:1B stoichiometry. *Nature* **420**, 193–198.

Zimmerman, A.L. & Baylor, D.A. (1992). Cation interactions within the cyclic GMP-activated channel of retinal rods from the tiger salamander. *Journal of Physiology* **449**, 759–783.

Zufall, F. & Munger, S.D. (2001). From odor and pheromone transduction to the organization of the sense of smell. *Trends Neuroscience* **24**, 191–193.